Modelling Measured 1/f Noise in Quanta Image Sensors (QIS)

Wei Deng[1] (Student), Dakota Starkey[1] (Student), Jiaju Ma[2] and Eric R. Fossum[1]

[1]Thayer School of Engineering, Dartmouth College, Hanover, NH, USA, [2]Gigajot Technology, Inc. Pasadena, CA, USA

Contact: Wei.Deng.TH@dartmouth.edu

Abstract─**We fit the measured in-pixel source follower (SF) 1/f noise using a modified mobility-fluctuation model [1] instead of the commonly-used model for analog designers [2]. Our model considers only mobility fluctuation as the origin of 1/f noise in our devices and includes correlated double sampling (CDS). The modeling results, using one adjustable parameter, match the experimental measurements, including the variation in noise from room temperature to -70C. This work provides useful information for the implementation of QIS in scientific applications and suggests even lower read noise is attainable by further cooling.**

I. INTRODUCTION

Quanta image sensor is proposed to be a next-generation solid-state image sensor. Compared to CMOS image sensors (CIS) and CCDs, QIS features high temporal-spatial resolution and single-photon sensitivity. It has been reported that a megapixel QIS is able to resolve photon number at room temperature without avalanche gain [3]. For accurate photon counting, the read noise target is below 0.15 e- rms [4]. Currently, noise from the in-pixel SF dominates the read noise of QIS and CIS. SF noise comes from different sources such as 1/f noise, random telegraph noise (RTN), and thermal noise. The origin of RTN is usually recognized as the trapping and de-trapping of conduction carriers, while theory of thermal noise is well-established. However, the origin of 1/f noise remains controversial.

Three well-known models have been developed to model 1/f noise, Hooge's mobility fluctuation model [5], McWhorter's number fluctuation model [6] and the Berkeley unified model [1]. Hooge's model is an empirical model which considers the origin as mobility fluctuation due to phonon scattering. Researchers tried to find the physical background of Hooge's alpha [7] but there is no widely-accepted explanation. McWhorter's model gained popularity after the discovery of RTN [8]. The combination of RTNs with a wide distribution of time constants yields a 1/f noise spectrum. However, as technology node scales further, researchers can easily observe the RTN induced by a single trap or several traps. Even for these RTN devices, the background noise after mathematically removing RTN still shows 1/f trend [9]. The Berkeley unified model considers number fluctuation and the correlated mobility fluctuation as the origin of 1/f noise. Different from the mobility fluctuation in Hooge's model which is a bulk effect, this model considers the mobility fluctuation induced by scattering from the charge near the Si-SiO$_2$ interface.

Since the very low sense node capacitance QIS is designed for single-electron charge sensitivity, RTS can be easily observed when present. However, there exists a lower-level of noise. From this, we speculate that the need for a mobility-fluctuation model to explain our measurements may be stronger than for other image sensor SFs, and perhaps there is more to SF background noise than just charge trapping (e.g., turbulent flow).

II. MODIFIED 1/F NOISE MODEL

The Berkeley unified model is originally proposed by K. K. Hung *et al.* in 1990. It considers both the carrier number fluctuation and the correlated surface mobility fluctuation. Since the number fluctuation is shown as RTN and is not likely the origin of 1/f noise, in our modified model, we only consider the contribution from the scattering-induced mobility fluctuation. The scattering is due to the charge near the Si-SiO$_2$ surface (trapped charge or surface charge). The 1/f noise power spectrum density (PSD) due to charge-scattering-induced mobility fluctuation is given by [1]

$$S_{I_b}(f) = \frac{kTI_b^2}{\gamma f W L^2} \int_0^L N_t(E_{fn})\,\alpha^2\mu^2 dx \qquad (1)$$

where k is Boltzmann constant, T is temperature, I_b denotes bias current, and γ is the attenuation coefficient of the electron wave function in the oxide, typically 10^8 cm^{-1} for Si-SiO$_2$ system. f is frequency. W and L are transistor width and length, respectively. $N_t(E_{fn})$ is trap density at quasi-Fermi level E_{fn}, α denotes scattering coefficient, and μ is electron mobility. Assuming $N_t(E_{fn})$ is uniform in space [1], the PSD can be simplified as

$$S_{I_b}(f) = \frac{kTI_b^2\alpha^2\mu^2 N_t}{\gamma f W L} \qquad (2)$$

Correlated double sampling is commonly used to reduce the reset noise from the pixel floating diffusion node. SF 1/f noise will be filtered by the correlated double sampling (CDS) circuitry. The CDS transfer function is given by [10]

$$H_{CDS}(f) = 2\sin(\pi f \Delta t) \qquad (3)$$

where Δt is the time difference between reset sampling and signal sampling. The dominant time constant due to

SF transconductance gm is denoted by $\tau_D = C_{col}/g_m$ where C_{col} is the column capacitance. SF functions as a low-pass filter and the cutoff frequency is given by $f_c = 1/(2\pi\tau_D)$. The transfer function (assuming gain is 1) can be written as

$$H_{LP}(f) = \sqrt{\frac{1}{1 + (f/f_c)^2}} \qquad (4)$$

The noise will be amplified by a programmable gain amplifier (PGA) with a switchable analog gain G_A before it is sent to the off-chip ADC. The SF 1/f noise power, due to the bandpass filtering and amplification, is hence given by

$$n_{1/f}^2 = \int_0^\infty \frac{S_{I_d}(f)}{g_m^2} H_{LP}^2(f) H_{CDS}^2(f) G_A^2 \, df \qquad (5)$$

Substituting (2), (3), (4) into (5), SF 1/f voltage noise can be written as

$$n_{1/f} = \eta G_A \frac{\sqrt{kT I_b \Psi(\pi f_c \Delta t)}}{W} \qquad (6)$$

where η is a mobility-dependent coefficient and is defined to be $\eta = \sqrt{\frac{2\alpha^2 \mu N_t}{\gamma C_{ox}}}$, G_A is switchable gain, and $\Psi(\pi f_c \Delta t) = \int_0^\infty \frac{\sin^2(\pi f_c \Delta t x)}{x(1+x^2)} dx$ is a function of the cutoff frequency f_c and CDS Δt [11].

III. CHARACTERIZATION RESULTS

Testing results from devices implemented in a TSMC 45/65nm stacked backside-illuminated (BSI) CIS baseline process [3] are presented. The noise for 4 types of SFs was measured, two buried-channel MOSFETs of different channel widths and two surface-channel MOSFETs of different channel widths (designated BC014, BC018, SC014, and SC020, where BC/SC denotes buried/surface channel and the number is the channel width, e.g. 014 means 0.14μm). The channel length is 0.27μm for all devices and a total of 1280 devices of each type were measured.

The QIS chip is shown in Figure 1, the schematic of the readout chain in Figure 2 and timing diagram in Figure 3. Figure 4 and 5 show the results from photon-counting histogram (PCH) testing using timing diagram Figure 2(a). The PCH of each jot was created by continuously measuring the jot output 20,000 times. The read noise and conversion gain were then extracted using valley-to-peak modulation (VPM) method [12]. Figure 4 shows the read noise histograms for jots with BC014 SF. The noise is notably smaller at -70C. Figure 5 shows a comparison between the BC014 SF and BC018 SF at -70C. Due to the smaller gate capacitance, the conversion gain of the jots with a BC014 SF is larger and therefore the FD-referred noise is lower.

1/f noise is measured by applying bandpass filtering using timing diagram Figure 2(b). The jot output was sampled by two CDS capacitors sequentially. The noise in different frequency regions is measured by adjusting CDS Δt [13]. During the testing, the chip was placed in a dark chamber, therefore the measured noise doesn't include photon shot noise. Instead, the total measured noise is mainly composed of SF noise and the kTC noise from the CDS capacitor. In 1/f noise analysis, only the quietest 1000 jots not showing RTN were analyzed for each type of SF [14]. The kTC noise from CDS capacitor, which is approximately equal to the measured noise when CDS Δt is 0, was subtracted in the analysis. The obtained SF noise is mainly 1/f noise since the SF thermal noise is much smaller after filtering.

Figure 6 shows comparisons between the modified Berkeley model and the experimental data. The noise shows a decreasing trend with smaller CDS Δt (consistent with [13]), smaller bias current, and lower temperature, as expected from the model. Moreover, noise is larger for smaller devices, which agrees with previous findings [1]. Buried-channel SFs have lower noise than surface-channel SFs likely due to less scattering. Table 1 shows the fitted η with 1μA bias current at -70C. The modeling reasonably matches the measurements, including temperature dependence, thus providing guidance to future cooled-temperature applications.

IV. SUMMARY

In this paper, a modified 1/f noise model which considers charge-scattering mobility fluctuation as the noise origin is introduced. Both modelled and measured 1/f noise are presented. This work suggests possible ways, either by bandpass filtering, SF sizing, or further cooling, to achieve even lower read noise and indicates possible QIS design and operation improvements for scientific applications.

REFERENCES

[1] K. K. Hung, P. K. Ko, C. Hu, and Y. C. Cheng, "A unified model for the flicker noise in metal-oxide-semiconductor field-effect transistors," IEEE Trans. Electron Devices, vol. 37, no. 3, pp. 654–665, 1990.
[2] N. Kawai and S. Kawahito, "Noise analysis of high-gain, low-noise column readout circuits for CMOS image sensors," IEEE Trans. Electron Devices, vol. 51, no. 2, pp. 185–194, Feb. 2004.
[3] J. Ma, S. Masoodian, D. Starkey, and E. R. Fossum, "Photon-number-resolving megapixel image sensor at room temperature without avalanche gain", OSA Optica, vol. 4, no. 12, pp. 1474-1481, Dec. 2017.
[4] E. R. Fossum, "Modeling the performance of single-bit and multi-bit quanta image sensors," IEEE J. Electron Devices Society, vol. 1, no. 9, pp. 166-174, Sept. 2013.
[5] F. N. Hooge. "1/f noise is no surface effect," Phys. Lett A 29.3 (1969): 139-140.
[6] A. L. McWhorter, "1/f noise and related surface effects in germanium," Ph.D. dissertation, MIT, Cambridge, MA, 1955.
[7] T. Musha, "Physical background of Hooge's α for 1/f noise," Phys. Rev. B 26.2 (1982): 1042.
[8] K. S. Ralls, W. J. Skocpol, L. D. Jackel, R. E. Howard, L. A. Fetter, R. W. Epworth, and D. M. Tennant, "Discrete resistance switching in

submicrometer silicon inversion layers: Individual interface traps and low-frequency (1/f?) noise," Phys. Rev. Lett. 52.3 (1984): 228.

[9] J. S. Kolhatkar, L. K. J. Vandamme, C. Salm, and H. Wallinga, "Separation of random telegraph signals from 1/f noise in MOSFETs under constant and switched bias conditions," in Proc. 33rd IEEE Conf. Eur. Solid-State Device Res., 2003, pp. 549–552.

[10] H. Wey and W. Guggenbuhl, "Noise transfer characteristics of a correlated double sampling circuit," IEEE Trans. Circuits Syst., vol. 33, no. 10, pp. 1028-1030, Oct. 1986.

[11]   A. Boukhayma, A. Peizerat, A. Dupret, and C. Enz "Comparison of two optimized readout chains for low light CIS", Proc. SPIE 9022, Image Sensors and Imaging Systems 2014, 90220H (4 March 2014).

[12] D. A. Starkey and E. R. Fossum, "Determining conversion gain and read noise using a photon-counting histogram method for deep sub-electron read noise image sensors," IEEE J. Electron Devices Society, vol. 4, no. 3, pp. 129–135, May 2016.

[13] C. Y.-P. Chao, H. Tu, T. Wu, K.-Y. Chou, S.-F. Yeh, and F.-L. Hsueh, "CMOS image sensor random telegraph noise time constant extraction from correlated to uncorrelated double sampling," IEEE J. Electron Devices Society, vol. 5, no. 1, pp. 79–89, 2017.

[14] W. Deng, D. Starkey, S. Masoodian, J. Ma, and E. R. Fossum "Quanta image sensors: photon-number-resolving megapixel image sensors at room temperature without avalanche gain", Proc. SPIE 10659, Advanced Photon Counting Techniques XII, 1065902 (14 May 2018).
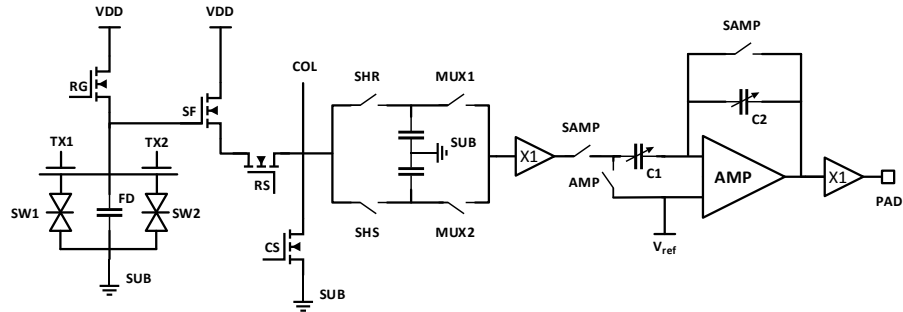
Figure 1. 20x1Mjot QIS test chip.

Figure 2. Schematic of the readout signal chain for analog output.
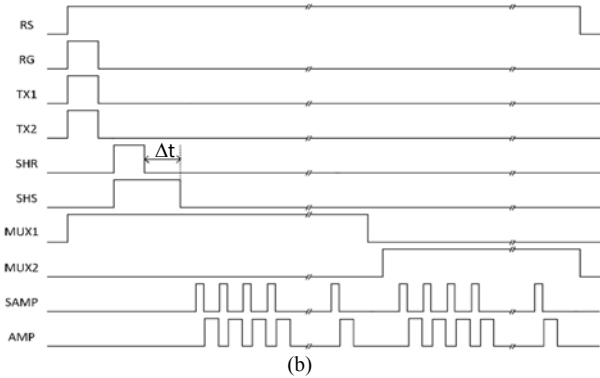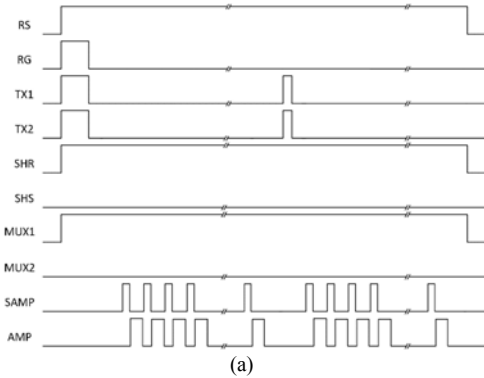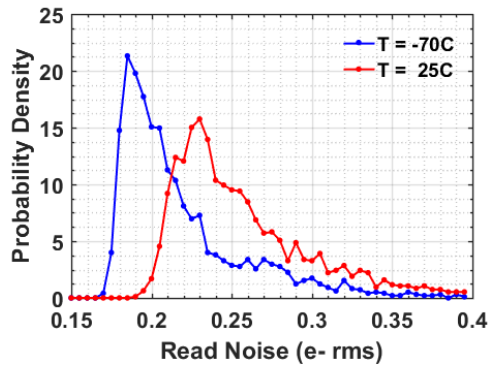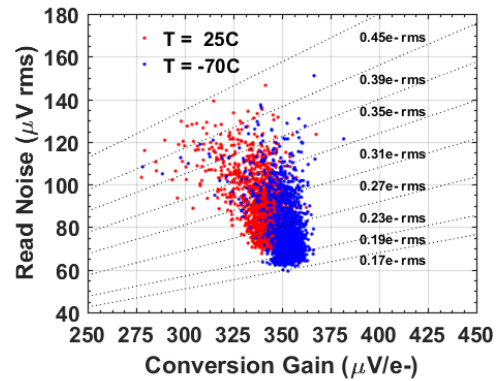

(a)

(b)

Figure 3. Timing diagram used for (a) photon-counting histogram testing and (b) SF noise testing.

(a)

(b)

Figure 4. (a) A histogram of the read noise of the jots (256x8) at -70C and 25C with BC014 SF. (b) A scatter plot of the voltage-referred read noise versus conversion gain of jots at -70C and 25C. (A small fraction of data with noise higher than 0.45 e- rms is not shown.)
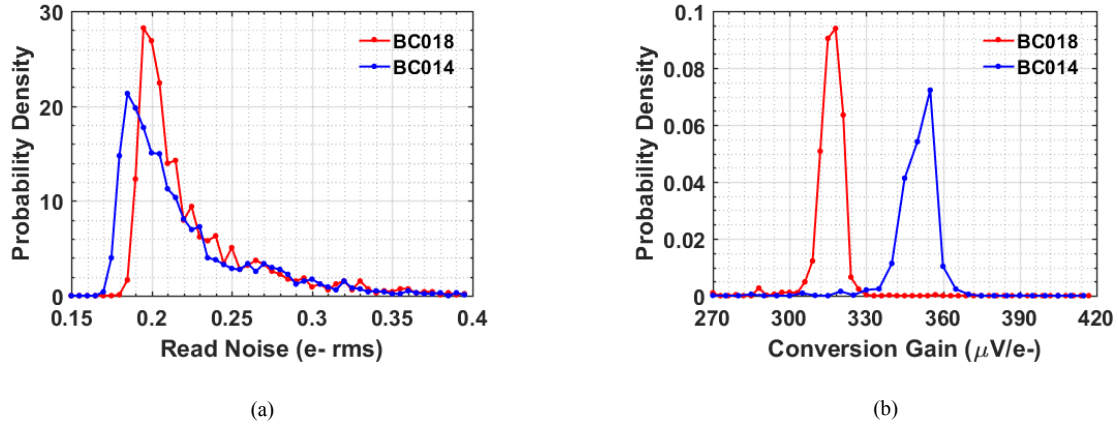
(a)

(b)

Figure 5. (a) A histogram of the read noise of the jots (256x8) with BC018 SF and BC014 SF at -70C. (b) A histogram of the conversion gain of the jots with BC018 SF and BC014 SF at -70C.
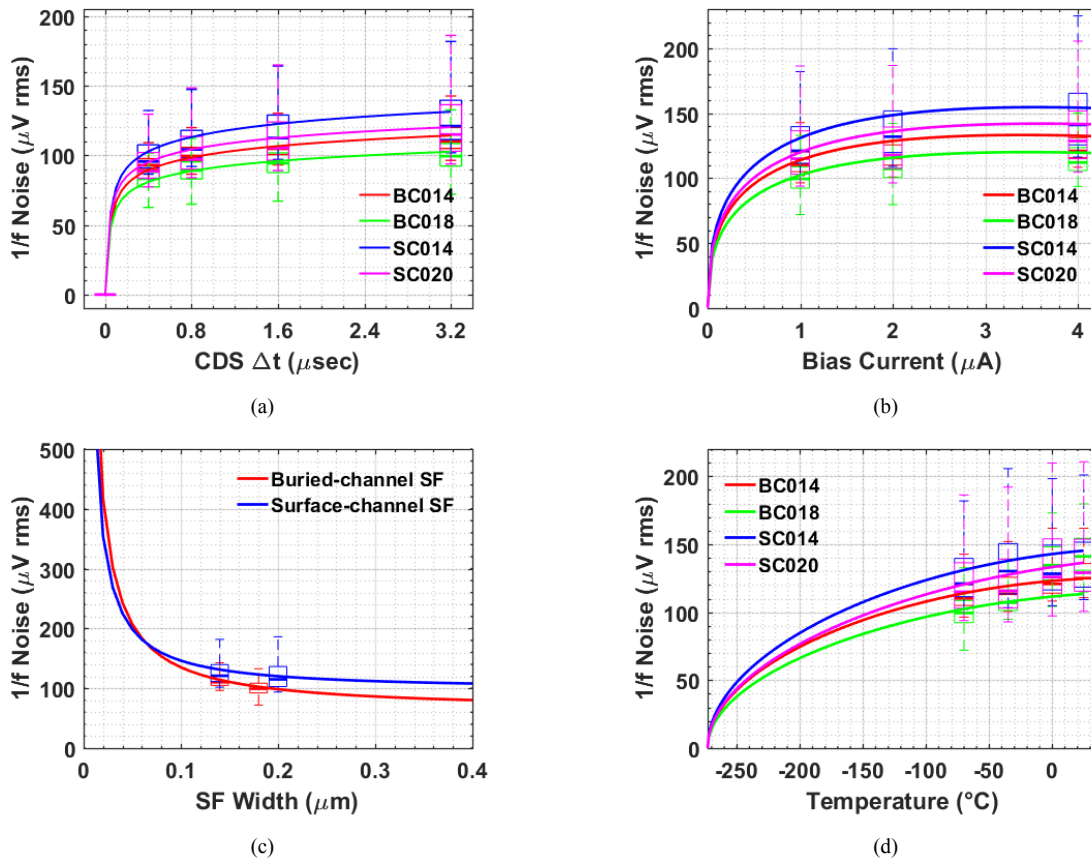

(a)

(b)

(c)

(d)

Figure 6. Modelled (using average noise) and measured noise for 4 types of SFs. (a) noise versus CDS Δt at temperature T = -70C and bias current I_b = 1µA. (b) noise versus bias current at temperature T = -70C and CDS Δt = 3.2µs. (c) noise versus SF transistor width at temperature T = -70C, I_b = 1µA and CDS Δt = 3.2µs. (d) noise versus temperature for 4 types of SFs at I_b = 1µA and CDS Δt = 3.2µs. The measured data is shown using filled circles and the simulated data is shown by solid lines.

Table 1. Extracted η at temperature T = -70C and bias current I_b = 1µA

SF type	BC014	BC018	SC014	SC020
$\eta\ (V \cdot m/\sqrt{J \cdot A})$	18.40	21.00	21.15	27.23